



Received: 2017.01.07
Accepted: 2017.02.03
Published: 2017.11.17

Authors' Contribution:

- A** Study Design
- B** Data Collection
- C** Statistical Analysis
- D** Data Interpretation
- E** Manuscript Preparation
- F** Literature Search
- G** Funds Collection

Multidetector Computed Tomography (CT) in Evaluation of Congenital Cyanotic Heart Diseases

Moanes M. Enaba¹□, Doaa I. Hasan¹□, Ahmed M. Alsowey¹□, Hany Elsayed²□

¹ Department of Radiodiagnosis, Zagazig University, Zagazig, Egypt

² Department of Pediatrics, Zagazig University, Zagazig, Egypt

Author's address: Moanes M. Enaba, Department of Radiodiagnosis, Zagazig University, Zagazig, Egypt,
e-mail: moanes_enaba@yahoo.com

Background:

The aim of the study is to emphasize the role of 128 MSCT angiography in the diagnosis of congenital cyanotic heart diseases.

Material/Methods:

This study included sixty patients and was conducted from December 2014 to July 2016 in the Multidetector CT unit of Zagazig University hospitals. All images included axial, MPR, MIP, and VRT and were interpreted in one session. Pulmonary veins were assessed for PAPVR or TAPVR, PDA, cardiac apex and heart chambers, interatrial or interventricular septal defects, pericardium, and site and size of the great veins (IVC and SVC).

Results:

This study included 60 patients. Thirty-four were boys (56.7%), and 26 were girls (43.3%). The age ranged from nine months to five years, and the mean age was 34.5 months. We found the following anomalies: tetralogy of Fallot (15 patients, 25%), tricuspid atresia (12 patients, 20%), Ebstein's anomaly (4 patients, 6.5%), pulmonic atresia or stenosis (7 patients, 11.5%), truncus arteriosus (6 patients, 10%), TGA (10 patients, 17%), and TAPVR (6 patients, 10%).

Conclusions:

MDCT proved to be an important modality for decision-making in patients with congenital cyanotic heart diseases.

MeSH Keywords:

Cyanosis • Heart Diseases • Multidetector Computed Tomography

PDF file:

<http://www.polradiol.com/abstract/index/idArt/903222>

Background

Congenital heart diseases (CHDs) are considered as the most common congenital birth defects, comprising 1% of all live births [1]. CHDs have two types, acyanotic and cyanotic, depending on the presence or otherwise of cyanosis on physical examination. In cyanotic CHDs, systemic venous blood bypasses the pulmonary circulation and gets shunted into the left half of the heart. The most important cyanotic CHDs include the so-called "5 Ts"; i.e., tetralogy of Fallot, truncus arteriosus, tricuspid atresia, transposition of the great arteries (TGA), and total anomalous pulmonary venous connection (TAPVR) [2]. The classic symptom of cyanotic CHDs is a bluish coloring of the skin. This usually occurs in the toes, fingers, and lips [3].

Echocardiography is the initial imaging modality for the assessment and diagnosis of CHDs. This method is operator dependent and limited by an acoustic window [4].

Traditional angiography is typically utilized as the gold standard modality for diagnosing CHD, but it has some limitations; it is invasive, requires general anesthesia, and is associated with exposure of neonates to radiation and iodinated contrast agents [5].

After recent developments in CT and MR technologies, cardiac catheterization is no longer necessary for diagnosis [6].

Multi-detector computed tomography (MDCT) can show the morphology of extra-cardiac vasculature, including the coronaries, pulmonary arteries, aorta, and pulmonary or systemic veins, and it delineates vessel walls and also

displays the airway, mediastinal abnormalities, and pulmonary parenchyma [7].

Aim of the work

The aim of the study is to emphasize the role of 128 MSCT angiography in the diagnosis of congenital cyanotic heart diseases.

Material and Methods

Patients

This study included 60 patients and was conducted from December 2014 to July 2016 in the Multidetector CT unit of the Zagazig University hospitals.

Inclusion criteria

Neonate or child with a clinical presentation of cyanosis and suspicion of CHD.

Exclusion criteria

Kidney disease associated with other causes, like contrast medium allergy, and orthopnea.

Ethical consideration

The protocol and informed consent forms used in the study were approved by the Institutional Review Board (IRB) of Zagazig University. All parents signed a written informed consent and filled a written survey including demographic and clinical data.

Patients were referred from the Department of Pediatrics. The age of patients ranged from 9 months to 5 years.

All patients were evaluated for:

1. **Medical history:** cyanosis and chest symptoms (cough, wheezes, and fever).
2. **Symptoms:** onset, course, duration, and distribution of cyanosis.
3. **Clinical findings on a physical examination.**
4. **Laboratory abnormalities: Kidney function tests:** BUN and serum creatinine.
5. **Structural defects of the heart – cardiac imaging studies including MDCT and echocardiography.**

Technique of MDCT

All MDCT evaluations were preceded by consultations with our colleagues from the Department of Pediatrics. Most of the studies were performed to answer particular anatomic inquiries raised by uncertain echocardiographic or angiographic assessments.

In pediatric patients who needed sedation, we orally administered chloral hydrate (50–100 mg/kg) and, if necessary, patients underwent intravenous sedation for 4–5 min that was supervised by an anesthesiologist.

Nonionic contrast medium was given intravenously via 20–22 G catheter with power dual injector at a rate of 1.5–4 mL/s and followed by a saline chaser; dose, 1–2 mL/kg; iodine concentration, 240–320 mg/mL. The bolus tracking marker was placed on the anatomic site of clinical relevance.

We used low radiation dose techniques; 25 mAs were used for patients younger than three years; 80 mAs for patients with body weight from 25 to 55 kg; 100–140 mAs for patients with body weight more than 55 kg; 60 kV for patients with body weight less than 45 kg; and 100–120 kV for patients weighing more than 45 kg. The thickness of the slice was 1.5 mm with a pitch of 1. The acquired axial slices were reconstructed in both sagittal and coronal planes. Furthermore, MPR, MIP, and VR were used. Exams started from the root of the neck, for the evaluation of supra-aortic arch branches, to below the diaphragm. If the aorta, veins, or abdominal organs were of interest, scanning was extended down to the pelvis. The time of exam was 5–12 s. Radiologists had access to unlimited numbers of reconstructed images in two workstations (volume navigator and volume wizard), they reviewed images and could rotate images to evaluate the organ of interest from any view. The images contained all anatomical data of the thorax, including the aorta and its branches, pulmonary artery and its branches, pulmonary veins, SVC, IVC, and other veins, cardiac chambers, pericardium, lung parenchyma, trachea, main tracheal bifurcation and main bronchus, ribs, abdominal organs, abdominal vessels, and visceral situs.

Studies interpretation

All images were assessed by a radiologist and a cardiologist. Image sets were systematically interpreted for supra-aortic arch branches, aorta from the beginning to the bifurcation - for the assessment of aortic position, coarctation, interruption, and collateral branches. The pulmonary trunk and its branches were assessed for their site, diameter, and junction of the two main branches. Evaluation of collateral vessel branches varied with patient age. The raters were blinded to the results of other imaging modalities. All images included axial, MPR, MIP, and VR and were interpreted in one session. Pulmonary veins were assessed for partial or total anomalous pulmonary venous return (PAPVR or TAPVR), patent ductus arteriosus (PDA), ASD, and VSD.

Transthoracic echocardiography (TTE)

TTE was performed in all patients before MDCT. The examination protocol included two-dimensional and Doppler imaging (parasternal, suprasternal, subxiphoid, and apical views). All echocardiograms were reviewed by an experienced pediatric cardiologist with particular attention to the vascular anomalies.

Statistics

Statistical analysis was performed with the SPSS software, version 17.0. We used Kappa test. Results were expressed as means \pm standard deviations for quantitative variables and as frequencies or rates for all other variables.

Table 1. Age (in months) and sex distribution.

| Total | Girls | Boys | Age |
|-----------|-----------|-----------|--------------|
| 22 | 10 | 12 | 0: <12 M |
| 10 | 6 | 4 | 12 M: <24 M |
| 15 | 6 | 9 | 24 M: <36 M |
| 8 | 3 | 5 | 36 M: <48 M |
| 5 | 1 | 4 | 48 M: 60 M |
| 60 | 26 | 34 | Total |

Results

Our study included 60 patients. Thirty four were boys (56.7%), and 26 were girls (43.3%). The age of patients ranged between nine months and five years, with the mean of 34.5 months (Table 1).

All patients presented with cyanosis and were suspected to have CHDs.

Cyanosis is a pale blue or purple staining of the mucous membranes and skin due to poor oxygenation. It is noticeable when the concentration of deoxygenated hemoglobin is greater than >5 g/dL, which is usually detected by pulse oximetry. Cyanosis is exceptionally hard to notice, unless arterial saturation is 85% or lower, and it is best found in the tongue and oral mucosa. Acrocyanosis (cyanosis limited to fingers and toes) is generally due to cooling and is considered as false cyanosis. Long-standing cyanosis causes finger clubbing.

Cardiovascular causes of cyanosis can be divided into ductal-dependent and ductal-independent lesions (Table 2). Ductal-dependent lesions require the ductus arteriosus for adequate pulmonary circulation, and they include tetralogy of Fallot (Figures 1, 2), Ebstein's anomaly, tricuspid atresia, and pulmonary atresia (or stenosis). Ductal-independent lesions result in pulmonary and systemic mixing that leads to deoxygenating of arterial blood, hence cyanosis. These lesions are TGA (Figure 3), TAPVR (Figure 4), and truncus arteriosus (Figure 5). In these conditions, blood mixing depends on ASD, patent foramen ovale (PFO), or VSD.

In all patients, full medical history was elicited (Table 3):

Cyanosis

- Either peripheral or central.
- Refractory cyanosis – not improved with oxygen treatment.

Fainting or cyanotic spells

- Exertional cyanosis, cyanosis following emotional disturbances, cyanosis after squatting due to dynamic obstruction of the right ventricular outflow tract, resulting in increased right-to-left intracardiac shunting (VSD, ASD)

Exercise intolerance

- History of exercise intolerance, including dyspnea on minimal exertion, or palpitations during physical effort.

Table 2. Cardiac causes of cyanosis.

| Ductal-independent lesions | Ductal-dependent lesions |
|---------------------------------|--|
| Truncus arteriosus | Tetralogy of Fallot |
| TGA | Tricuspid atresia or Ebstein's anomaly |
| TAPVR | Pulmonary atresia or stenosis |
| Hypoplastic left heart syndrome | |

Gestational history and family history

- Prenatal screening is important as some inborn/congenital syndromes are associated with congenital cardiac anomalies.
- Maternal illness, including diabetes, drugs that can be teratogenic, or rubella.
- Recently, those fetuses who are suspected to have cardiac abnormalities require an echocardiogram during pregnancy to look for cardiac defects of the fetus.
- Family history of congenital cardiac disease is important, as more and more people with congenital heart diseases reach reproductive age.

Physical examination (Table 4) was performed, including a complete examination of the heart and lungs.

Inspection

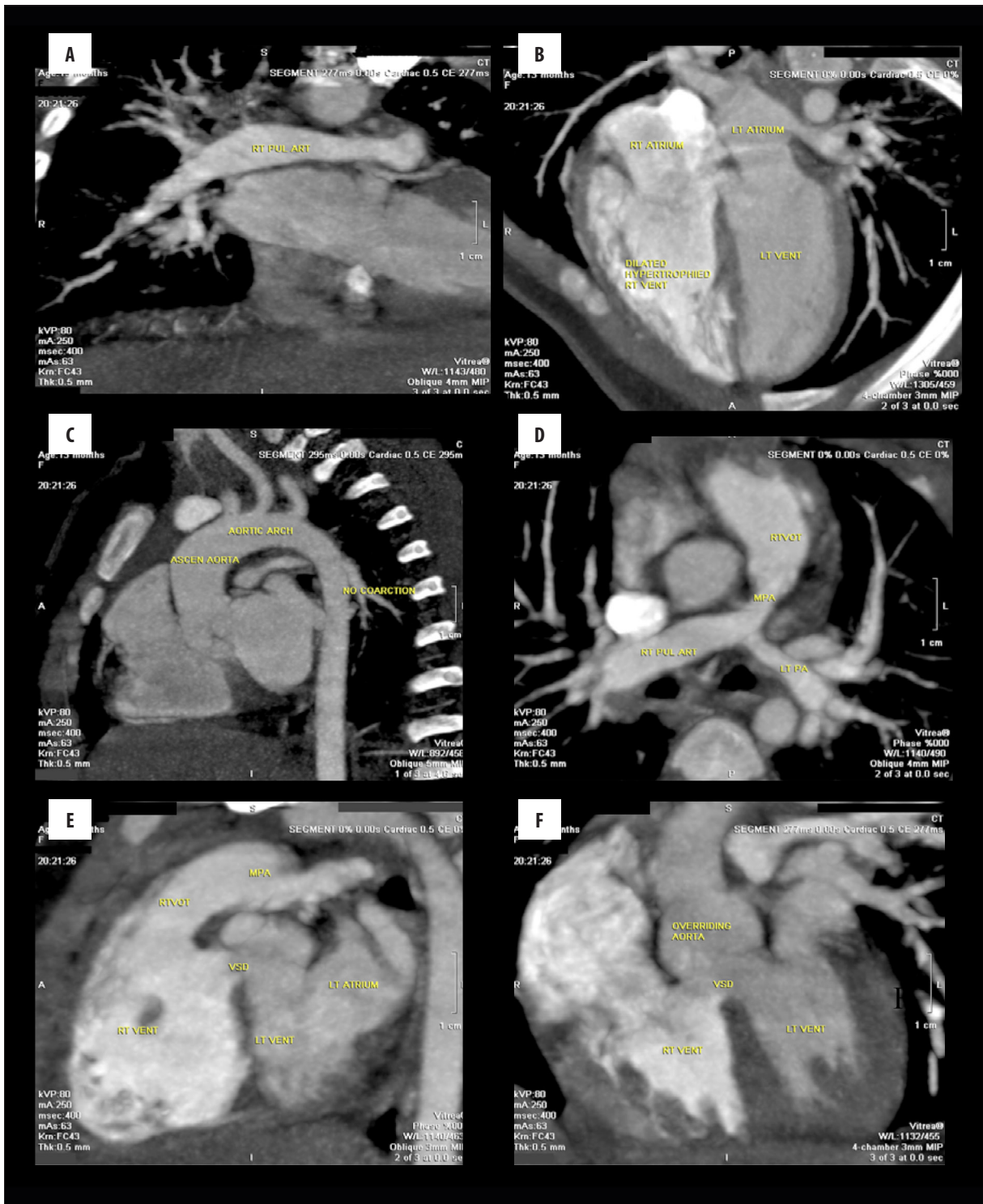
- Symptoms of genetic/congenital anomalies (Down's syndrome is accompanied by endocardial cushion defects, Turner's syndrome is accompanied by coarctation of aorta)
- Detection of cyanosis - peripheral or central.
- Differential cyanosis.

Cardiac examination

- Cardiac pulsations, pulse oximetry, palpation of peripheral pulses, and measurement of blood pressure.
- Auscultation for murmurs.
- Signs of heart failure: hepatomegaly and edema of lower limbs

Respiratory examination

- Signs of respiratory distress such as tachypnea, dyspnea.
- Palpation for asymmetric diaphragmatic elevation, and percussion for consolidation, pleural effusions, and pneumothorax.



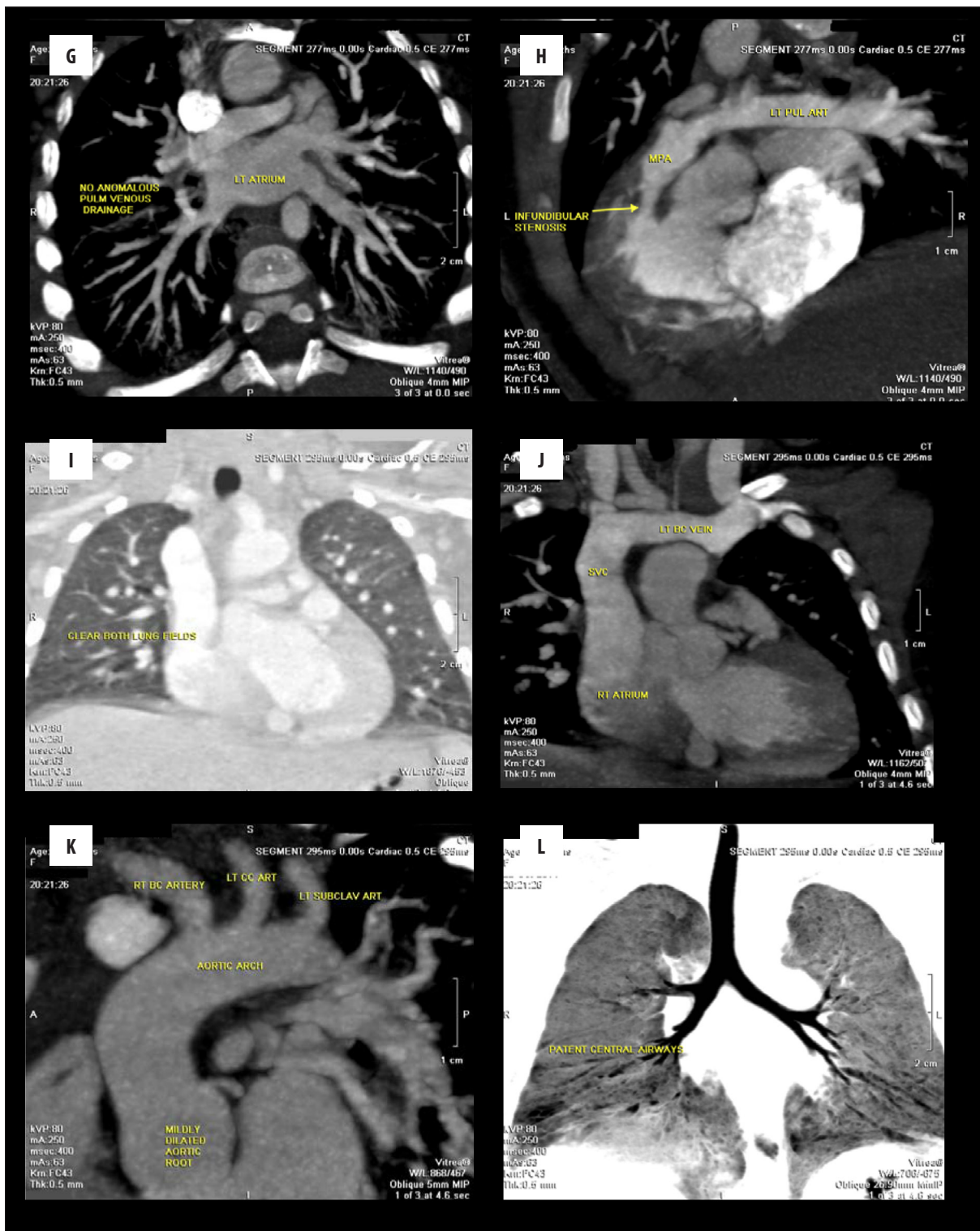
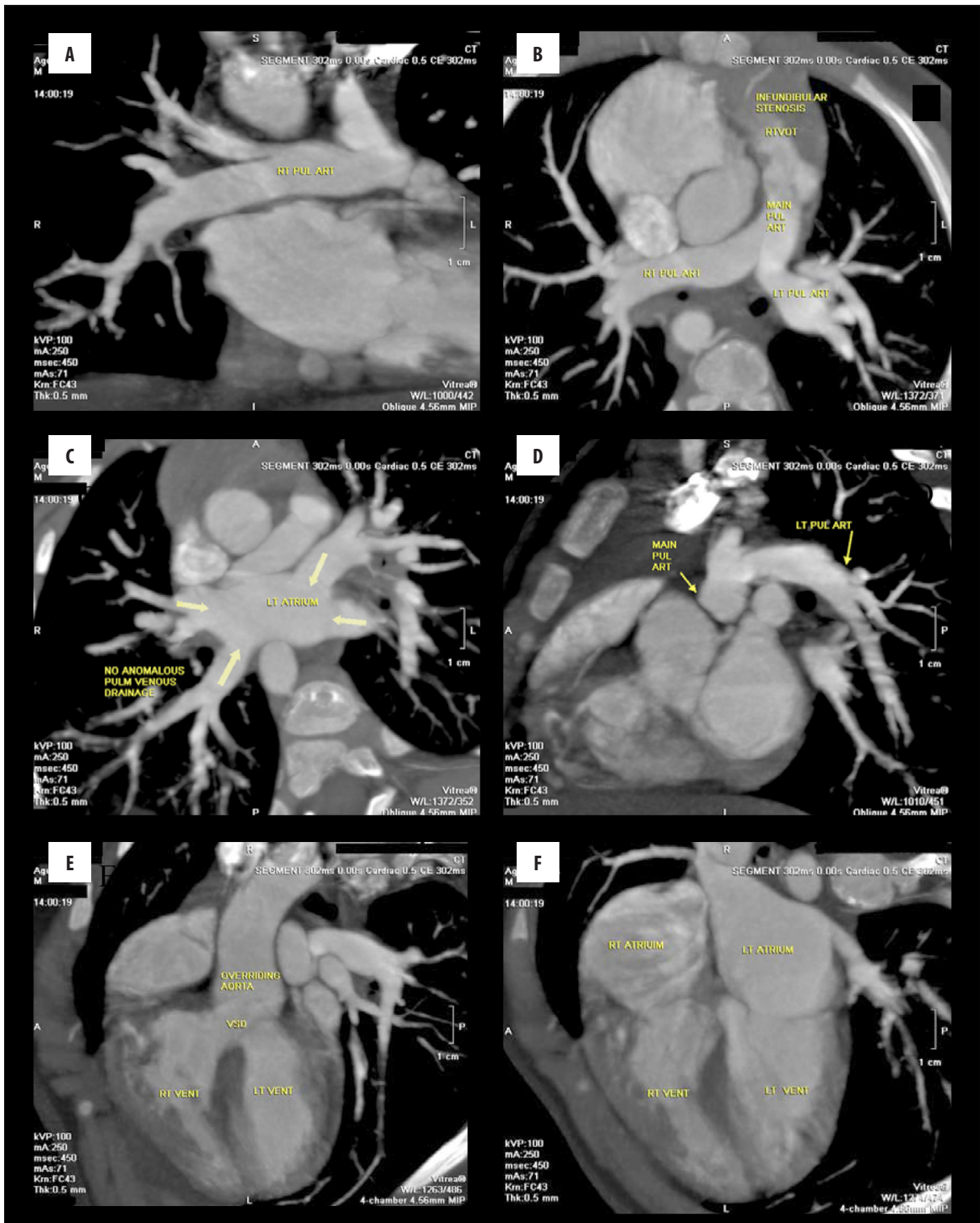


Figure 1. 128-MDCT angiography of the heart and great vessels (multiple axial, coronal, and sagittal cuts) of a female patient (13 months of age) diagnosed with tetralogy of Fallot (TOF); the examination revealed course of the right pulmonary artery (A), dilated and hypertrophied right ventricle (B, J) with increased mural wall thickness, VSD (E, F), overriding of the aorta (F) without coarctation (C), infundibular pulmonary stenosis (H), mildly dilated aortic root (K) with no anomalous pulmonary venous drainage (G) surrounding both lung fields (I), and patent central airways (L).



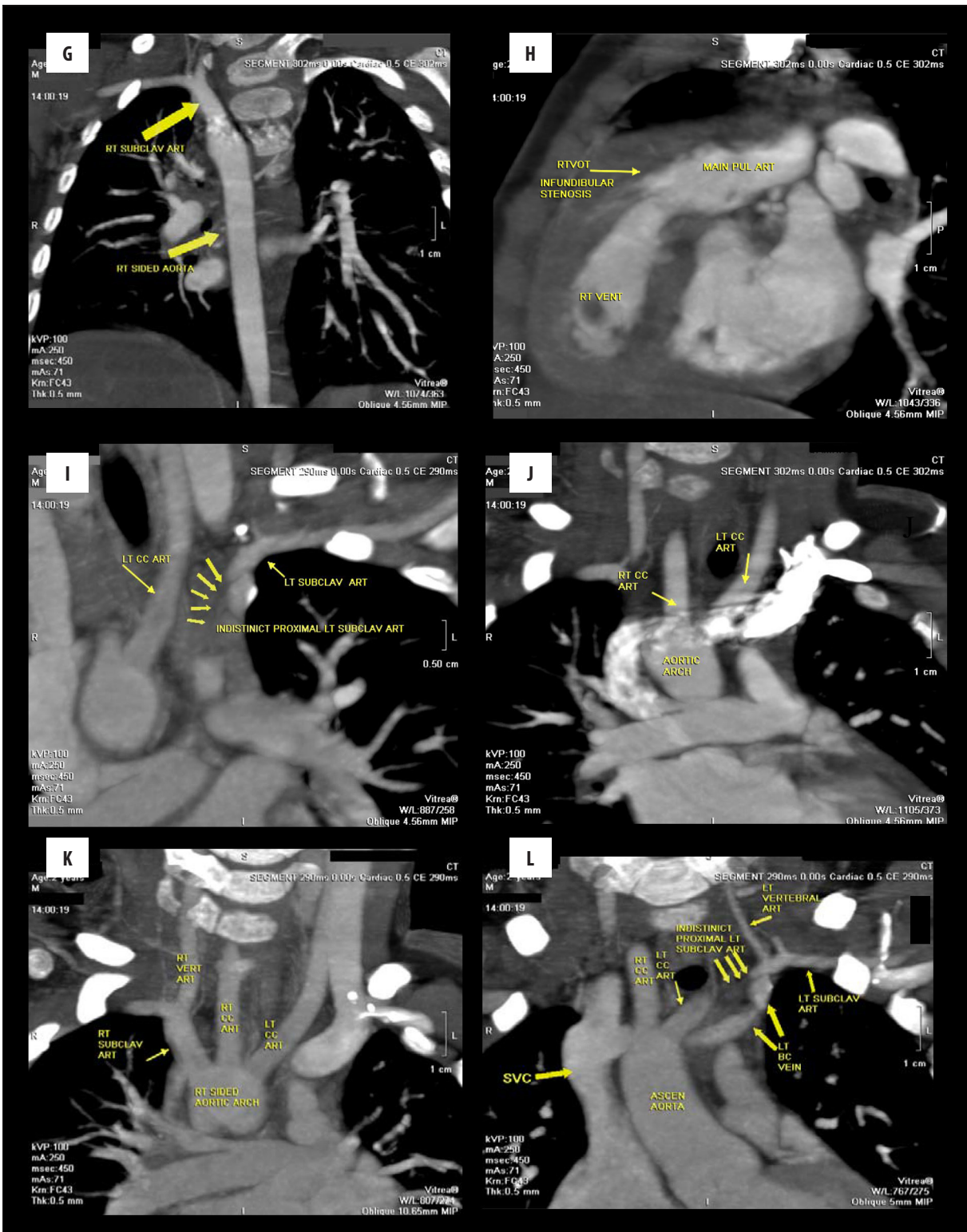
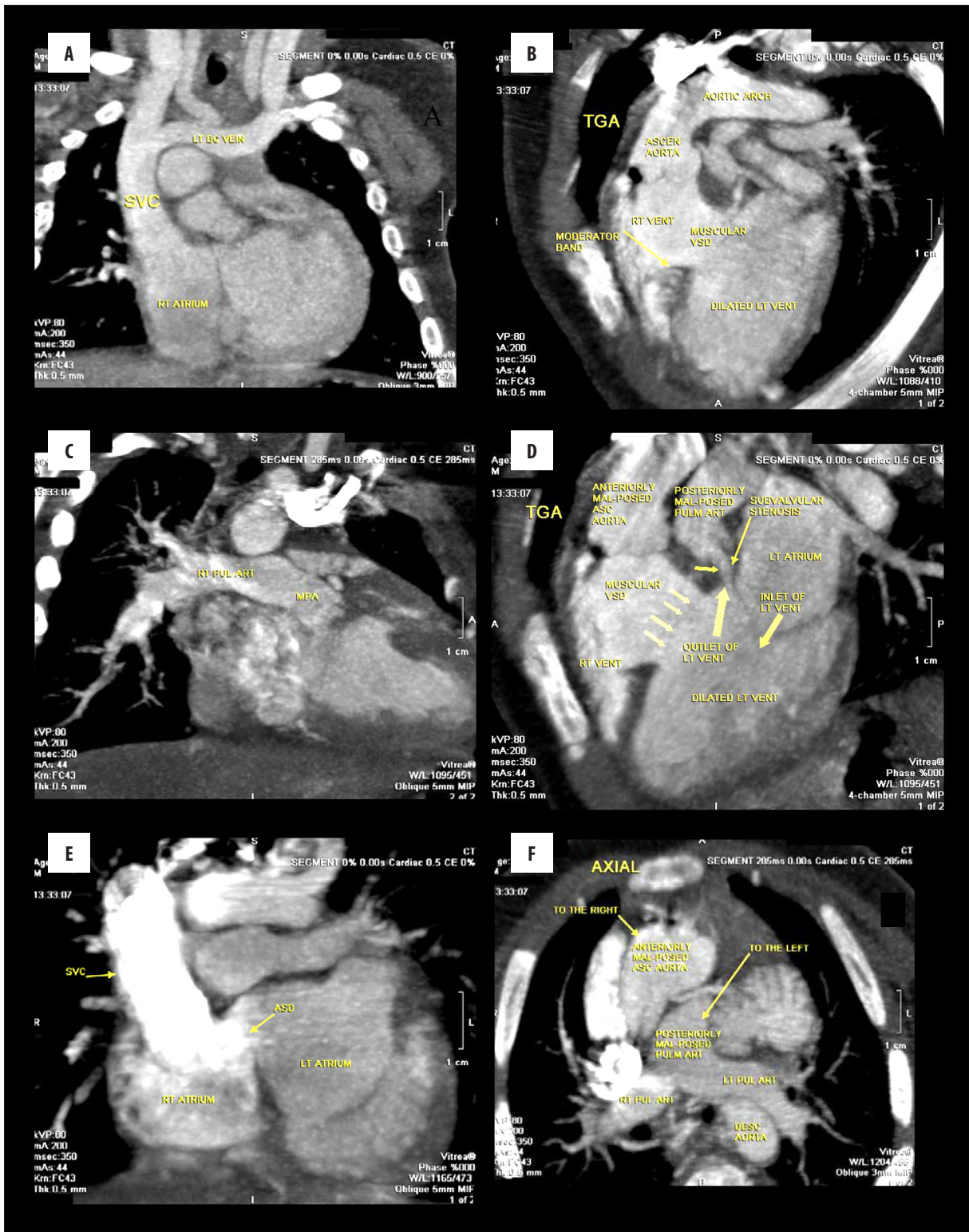


Figure 2. 128-MDCT (multiple axial, coronal, and sagittal cuts) of a male patient (2 years of age) diagnosed with tetralogy of Fallot (TOF); the examination revealed course of the right pulmonary artery (A), dilated and hypertrophied right ventricle (E, F, H), infundibular stenosis (B, H), VSD (E) overriding the aorta (E), right-sided aortic arch (G, K), and indistinct proximal left subclavian artery (I, L) with no anomalous pulmonary venous drainage (C).



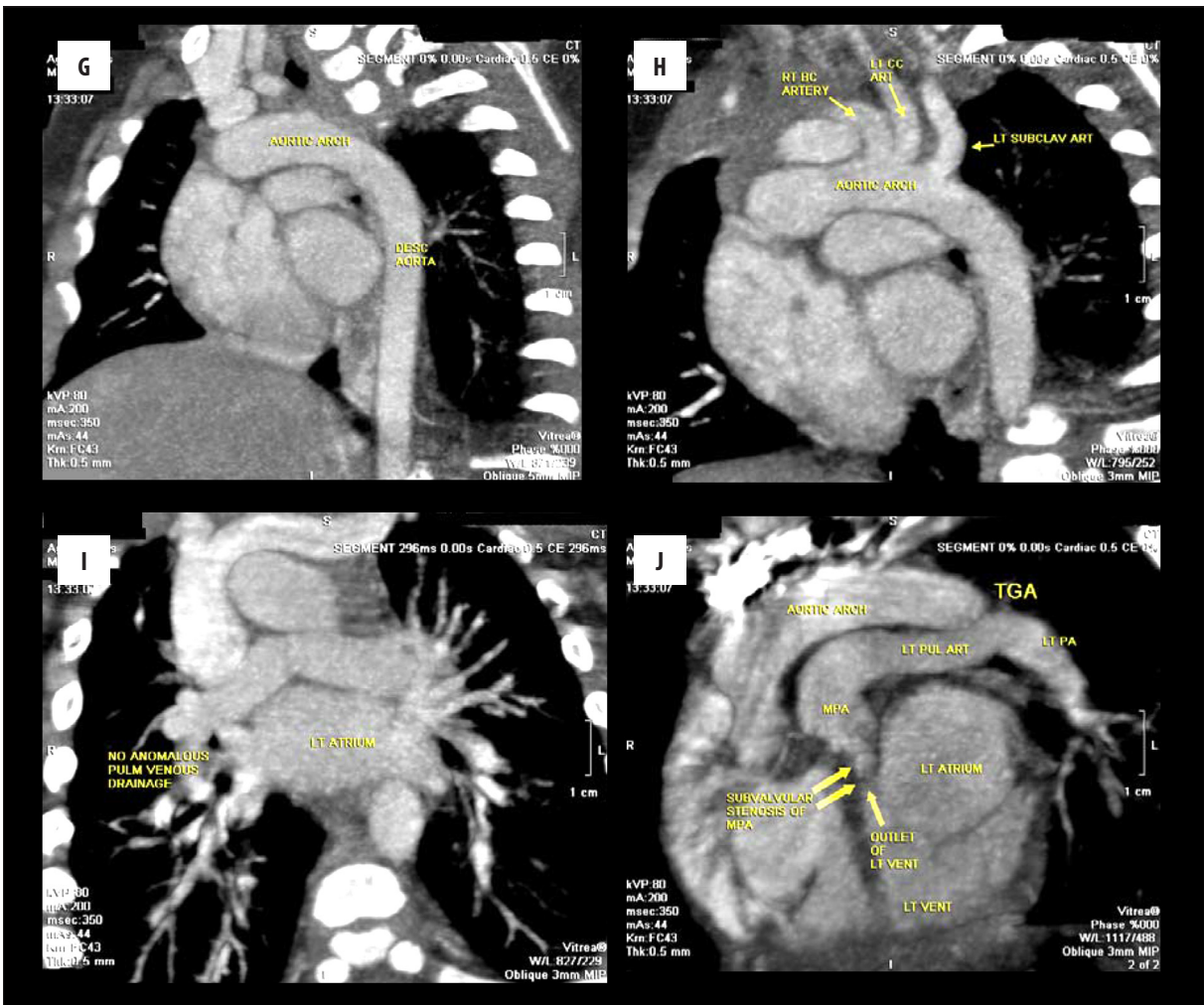


Figure 3. 128-MDCT (multiple axial, coronal, and sagittal cuts) of a male patient (5 years of age) diagnosed with TGA; the examination revealed SVC and right atrium (A), ascending aorta originating from a dilated right ventricle (B); the main pulmonary artery is seen originating from the dilated left ventricle with sub-valvular pulmonary valve stenosis (D, J), muscular VSD (D), anteriorly malpositioned ascending aorta to the right side (F), posteriorly malpositioned pulmonary artery to the left side (F), ASD (E) with no anomalous pulmonary venous drainage (I).

Table 3. Clinical history of patients.

| Patient symptoms | No. of patients |
|-----------------------|-----------------|
| Cyanosis. | 60 |
| Cyanosis on exertion. | 12 |
| Exercise intolerance. | 32 |
| Palpitation. | 26 |

The same patient could presented with one or more symptoms.

- Auscultation for air entry, crackles (to evaluate if there are effusions or consolidations)
- Congestive heart failure: dullness at the lung bases in case of pleural effusion, basal crackles in case of pulmonary edema.

Chest X-ray (CXR)

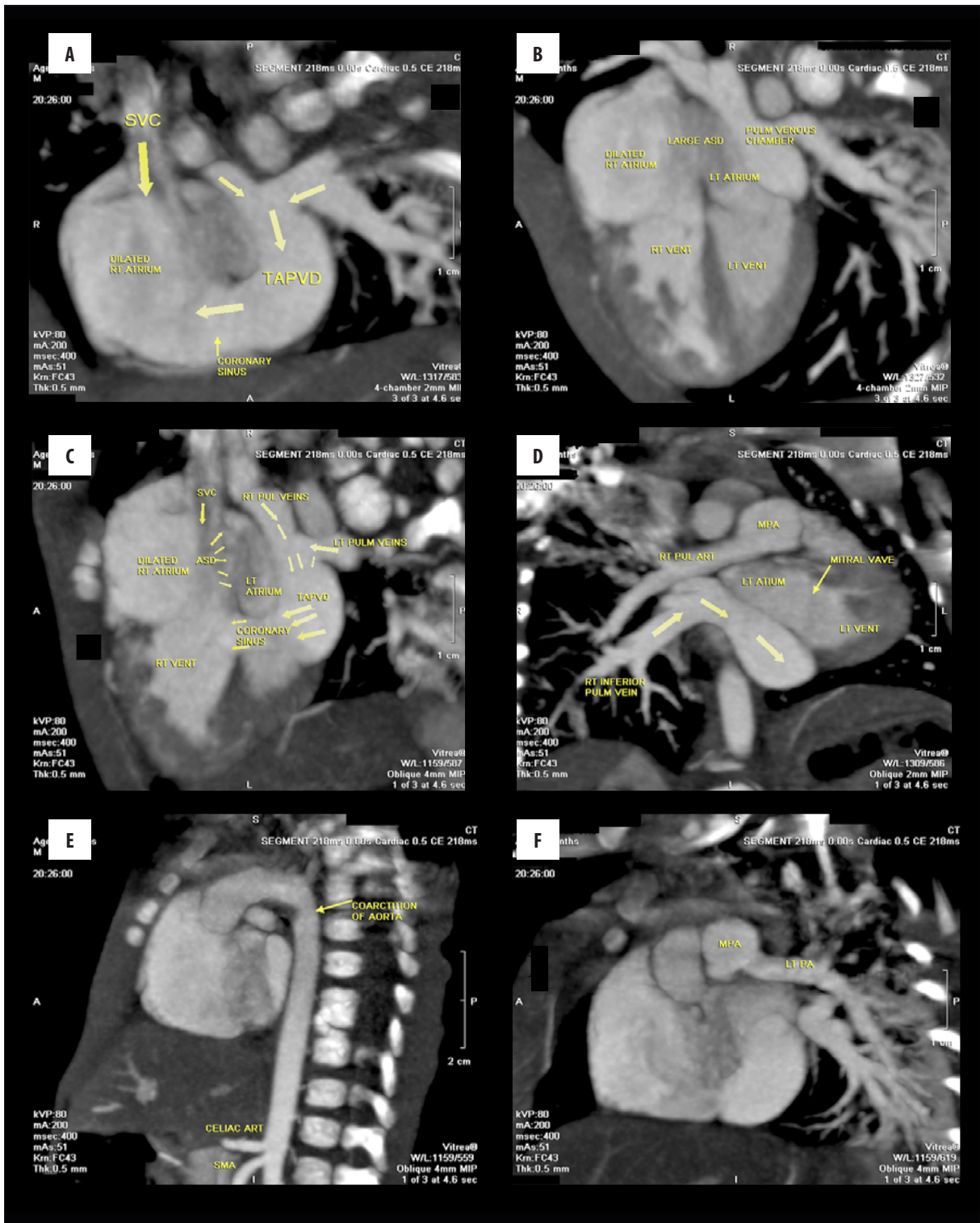
Chest x-ray is helpful to show heart size and pulmonary vessels.

Table 4. Physical examination.

| Signs of examination | No. of patients |
|-----------------------|-----------------|
| Peripheral cyanosis | 12 |
| Central cyanosis | 56 |
| Differential cyanosis | 32 |
| Tachycardia | 32 |
| Tachypnea | 44 |

The same patient could have one or more signs.

- Cyanotic cardiac lesions with high vascularity include simple TGA and TAPVR.
- Cyanotic cardiac lesions with low vascularity include complex TGA, TOF, and Ebstein’s anomaly, also tricuspid and pulmonary atresia.
- Certain unique chest x-ray findings might be helpful and include:
Egg-shaped heart in TGA.



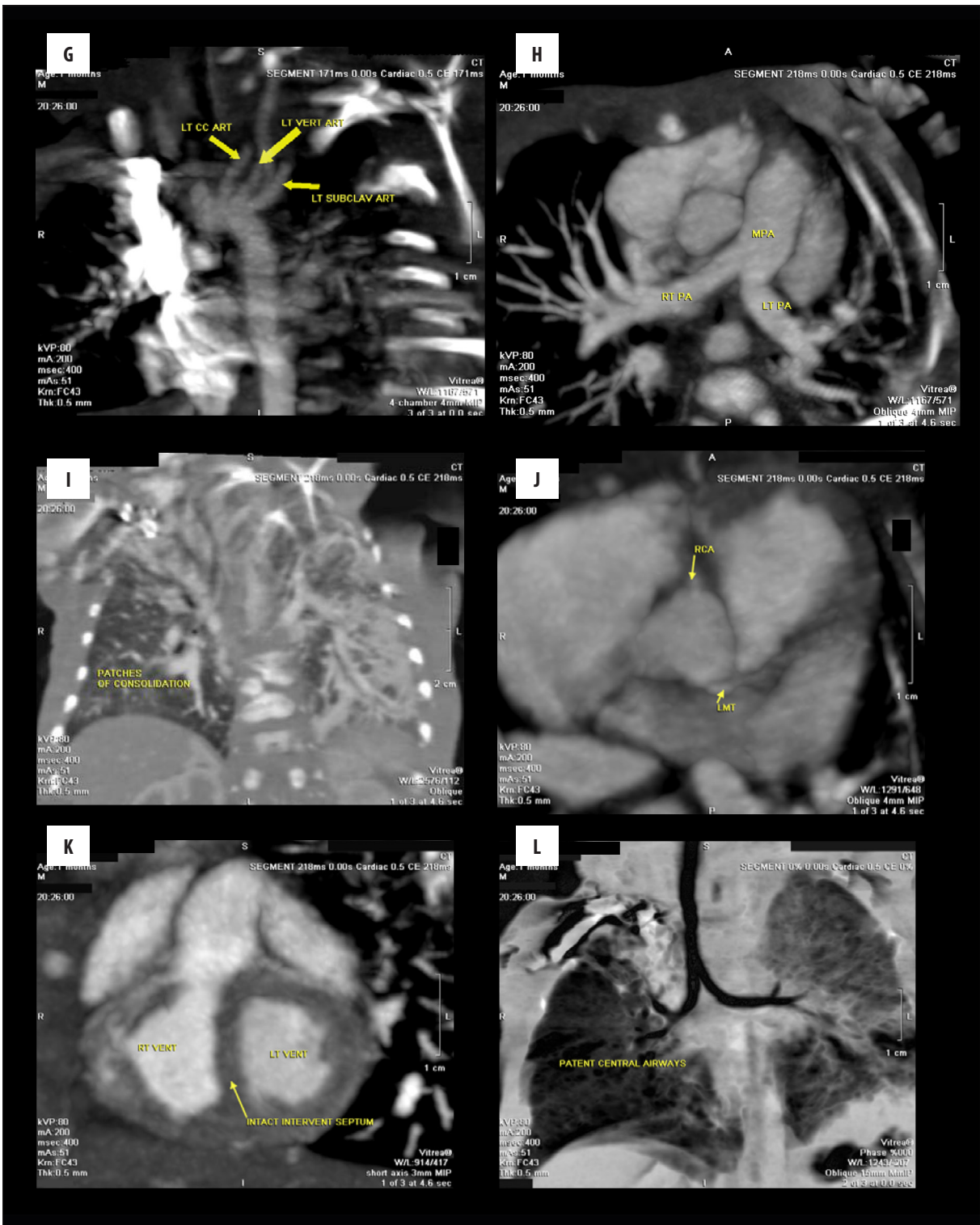
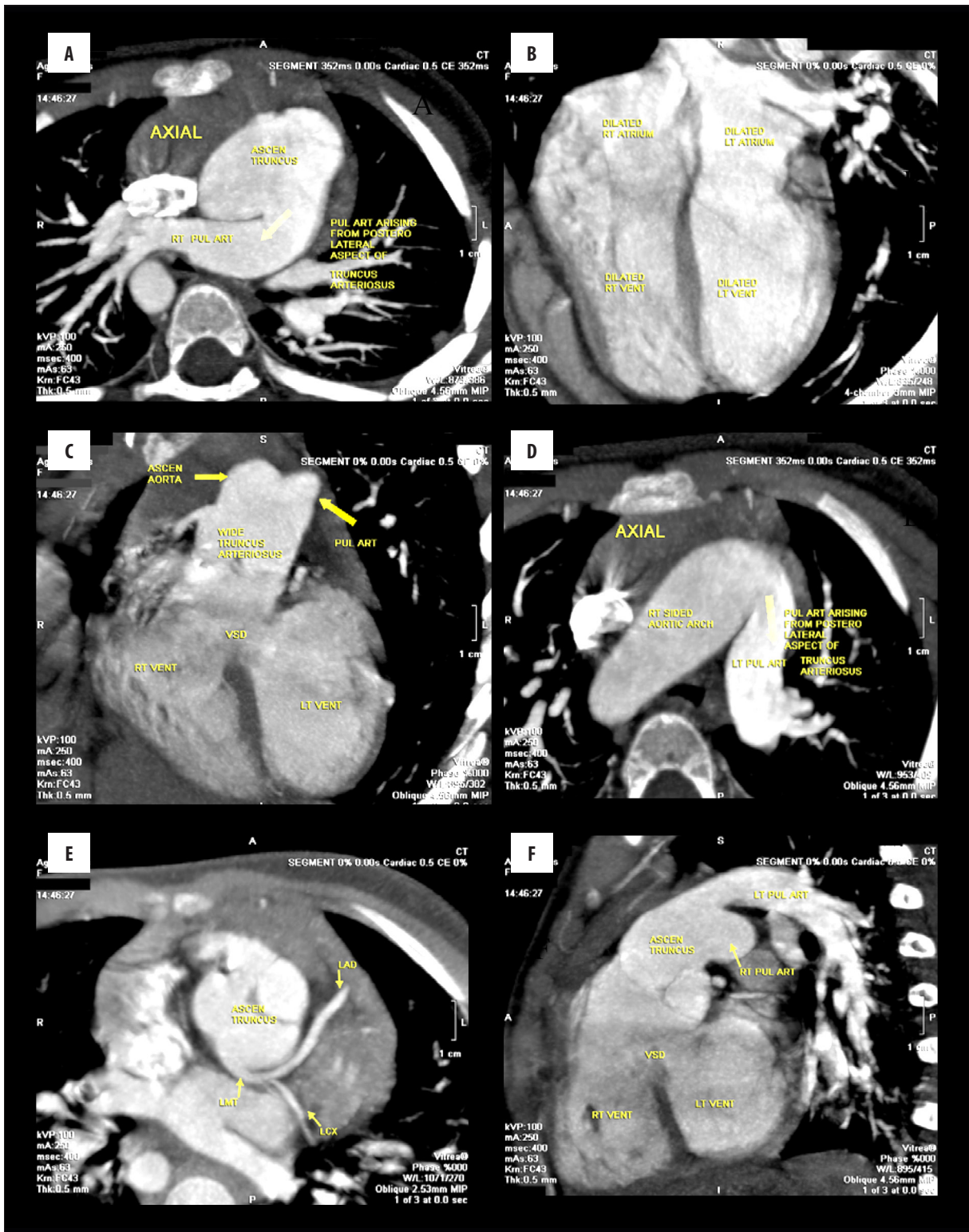


Figure 4. 128-MDCT (multiple axial, coronal, and sagittal cuts) of a male patient (1month of age) diagnosed with Type II TAPVR; the examination revealed pulmonary venous drainage into the right atrium via the coronary sinus (A–D), dilated right atrium (A, B), large ASD (B, C) with aortic coarctation (E), intact inter-ventricular septum (K). Bilateral patches of consolidations (I) with patent central airways (L).



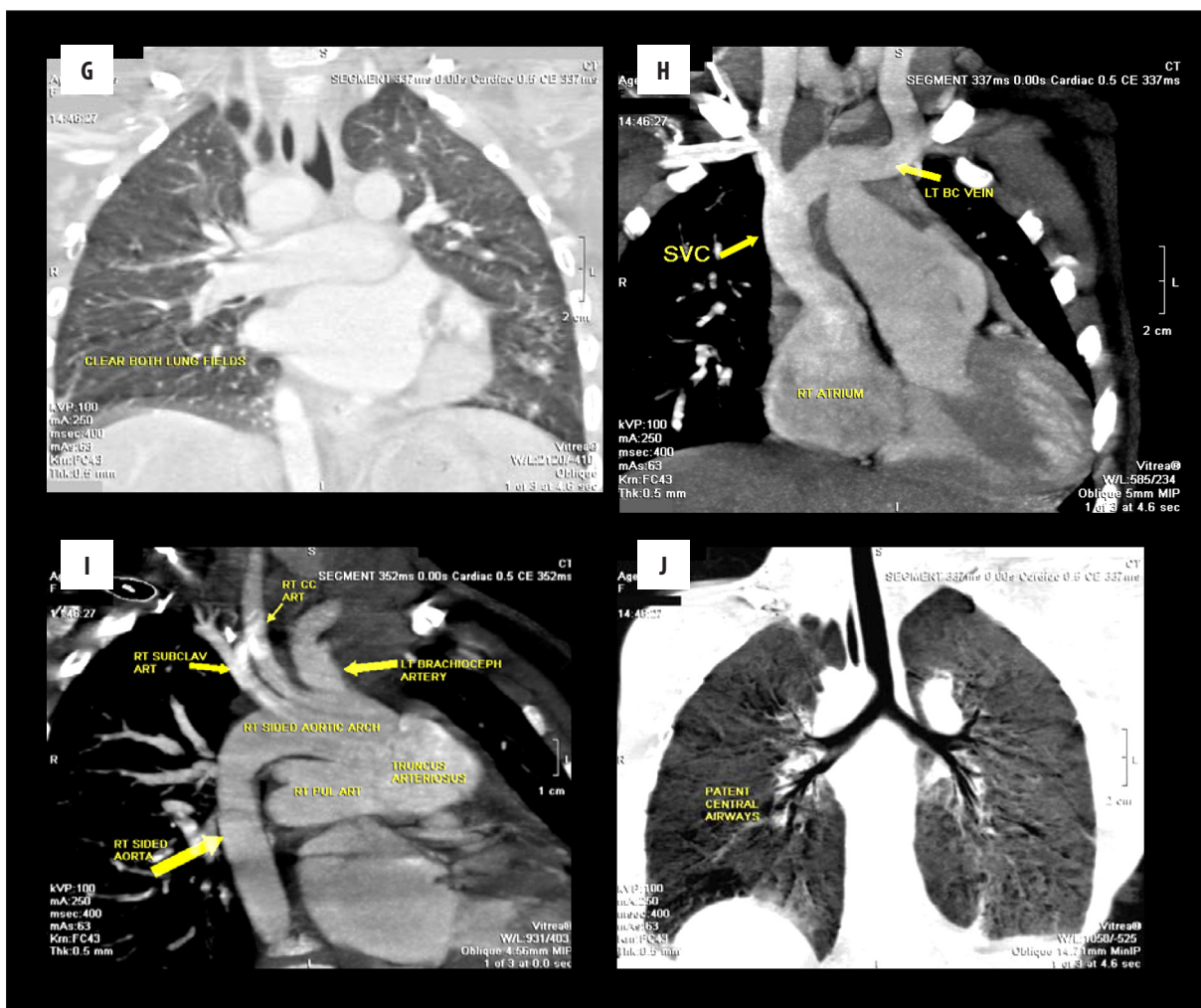


Figure 5. 128-MDCT (multiple axial, coronal, and sagittal cuts) of a female patient (4 years of age) diagnosed with truncus arteriosus (A); the examination revealed dilation of all cardiac chambers (B), pulmonary artery arising from the posterolateral aspect of the truncus arteriosus (A), VSD (C, F) and right-sided aortic arch (D, I) surrounding both lung fields (G), and patent central airways (J).

Table 5. Numbers of anomalies.

| Cardiac anomaly | No. of patients |
|-------------------------------|------------------|
| Tetralogy of Fallot | 15 (25%) |
| Tricuspid atresia | 1 (20%) |
| Ebstein's anomaly | 4 (6.5%) |
| Pulmonary atresia or stenosis | 7 (11.5%) |
| Truncus arteriosus | 6 (10%) |
| TGA | 10 (17%) |
| TAPVR | 6 (10%) |
| Total | 60 (100%) |

Boot-shaped heart in tetralogy of Fallot.
 Snowman appearance in TAPVR.
 Extreme cardiomegaly can occur in Ebstein's anomaly.
 All MDCT angiography studies were performed before any surgical correction.

MDCT findings

- To assess the basic components of Tetralogy of Fallot (Figures 1, 2)
- TGA (Figure 3)
- TAPVR (Figure 4).
- Truncus arteriosus (Figure 5)

The numbers of the anomalies in the study diagnosed by MDCT were as follows, tetralogy of Fallot (15 patients, 25%), tricuspid atresia (12 patients, 20%), Ebstein's anomaly (4 patients, 6.5%), pulmonary atresia or stenosis (7 patients, 11.5%), truncus arteriosus (6 patients, 10%), TGA (10 patients, 17%), and TAPVR (6 patients, 10%) (Table 5).

We compared the diagnostic value of MDCT and TTE. We found that sensitivity and specificity of MDCT in diagnosing Tetralogy Fallot were 91.2% and 98.2%, respectively; for diagnosing tricuspid atresia were 99.4% and 64.8%, respectively; for diagnosis Ebstein's anomaly were 96.9% and 90.8%, respectively; for diagnosing pulmonary atresia or stenosis were 98.2% and 95.5%, respectively, for diagnosing tricuspid atresia were 98.6% and 47.1%, respectively; for

Table 6. Final diagnoses based on both TTE and MDCT.

| Cardiac anomaly | Diagnosed by MDCT | Diagnosed by TTE |
|-------------------------------|-------------------|------------------|
| Tetralogy of Fallot | 15 | 13 |
| Tricuspid atresia | 12 | 10 |
| Ebstein's anomaly | 4 | 2 |
| Pulmonary atresia or stenosis | 7 | 5 |
| Truncus arteriosus | 6 | 4 |
| TGA | 10 | 10 |
| TAPVR | 6 | 4 |
| Total | 60 | 48 |

diagnosing transposition of great arteries were 98.9% and 95.5%, respectively; for diagnosing TAPVR were 97.7% and 95.5%, respectively.

We also measured the agreement between both tests (MDCT and TTE). There was very good agreement ($k=0.870$) in detecting major cardiac vascular lesions, and good agreement was seen for complex vascular anomalies ($k=0.776$). The agreement was fair for intra-cardiac anomalies ($k=0.571$). The P value was highly significant in both tests ($P=0.001$) (Table 6).

Discussion

The incidence of CHD is different in studies conducted in different countries [8]. Tetralogy of Fallot accounts for about 10% of cases of CHD [9]. TAPVR is an anomalous diversion of oxygenated blood into the systemic venous flow, in which mixed blood flows via ASD or PFO to systemic organs. TAPVR is noted in nearly 1.5% of all patients with cardiovascular anomalies and in 6.8 per 100,000 of live births. Anomalous venous communication can be cardiac, supracardiac, infracardiac, or mixed, depending on the sites of attachment, with the supracardiac communication being the commonest [10].

The role of MDCT in the detection of intra-cardiac anomalies is promising owing to the advances in MDCT scanners and ECG-gating techniques. In a small study with a 40-MDCT scanner (without ECG gating), Hayabuchia et al. [11] detected 53 of 54 intra-cardiac and extra-cardiac anomalies in neonates with CHD. CT examination is also valuable in the assessment of extracardiac systemic and pulmonary arterial and venous structures. For radiologists, it is essential to have exact information on cardiovascular anatomy, physiology, and surgical techniques [12].

Compared with old generation CT scanners, 128-slice MDCT or even better scanners yield images with better temporal and spatial resolutions, provide wider anatomic coverage per rotation, enhancement is seen with smaller volumes of injected contrast media, and a higher quality of multiplanar reconstructions and 3D reformations is possible owing to acquisition of an isotropic information set

[13]. Rapid imaging with these CT scanners could be done with a small dose of sedative, with shorter breath holding time than in old generation CT, MRI, or conventional angiography [14].

MDCT has several advantages. First, it permits to acquire high-definition images within seconds [10]. Furthermore, it allows imaging vascular structures as small as 1-2 mm. In cardiology, MDCT is the non-invasive first-line modality used for the detection of coronary abnormalities and other cardiac diseases [15]. Some studies pointed out that MDCT is also valid to study shunt-size, location, and flow direction. It is also the method of choice in patients with metallic devices and pacemakers [16]. MDCT also allows performing analyses of cardiac dimensions and function, with less definition for segmental contraction compared to MRI [17]. Function of prosthetic valves can also be assessed [18].

The main disadvantage of MDCT is radiation exposure, which must be taken into consideration, especially in children. There are no reliable epidemiologic investigations of malignancy risk associated with CT; however, radiation exposure should be as low as possible during scanning. We found that all clinically relevant diagnostic information can be obtained using low-dose, non-ECG-gated 128-MDCT. In comparison to catheter angiography, non-ECG-gated MDCT is a relatively static imaging method that is best suited for morphologic assessment. For functional evaluation, like ejection fraction and regional wall motion, ECG-gated images are required, which will considerably increase radiation exposure [19].

Conclusions

This article illustrates the use of 128-MDCT for a comprehensive evaluation of different anatomic structures, including the heart, pulmonary and systemic thoracic vasculature, and lungs in patients with congenital cyanotic heart diseases. MPR and 3D CT reformation images can improve visualization of anatomic points that are of interest to clinicians. MDCT has become a valuable imaging modality alongside echocardiography or as a substitute for invasive angiography in the assessment of patients with CHD.

References:

1. Madsen NL, Marino BS, Woo JG et al: Congenital heart disease with and without cyanotic potential and the long-term risk of diabetes mellitus: A population based follow up study: *J Am Heart Assoc*, 2016; 5: pii: e003076
2. Rao PS: Diagnosis and management of cyanotic congenital heart disease: Part I. *Indian J Pediatrics*, 2009; 76: 57–70
3. Ellis ME: Cyanotic congenital heart disease: <http://www.healthline.com/health/cyanotic-heart-disease#Symptoms4>, January, 2016
4. Park MK: *The pediatric cardiology handbook*. 4th Edition. Philadelphia: Mosby Elsevier; 2010
5. Rao PS: Diagnosis and management of cyanotic congenital heart disease: Part II. *Indian J Pediatrics*, 2009; 76(3): 297–308
6. Hellinger JC, Daubert M, Lee EY, Epelman M: Congenital thoracic vascular anomalies: evaluation with state-of-the-Art MR imaging and MDCT. *Radiol Clin N Am*, 2011; 49: 969–96
7. Bayraktutan U, Kantarci M, Ogul H et al: The utility of multidetector computed tomography for evaluation of congenital heart disease. *Folia Morphol*, 2013; 72(3): 188–96
8. Patel N, Jawed S, Nigar N et al: Frequency and pattern of congenital heart defects in a tertiary care cardiac hospital of Karachi. *Pak J Med Sci*, 2016; 3(1): 79–84
9. Ahmed S, Johnson PT, Fishman EK, Zimmerman SL et al: Role of multidetector CT in assessment of repaired tetralogy of fallot. *Radiographics*, 2013; 33(4): 1023–36
10. Al-Mousily F, Shifrin RY, Fricker FJ et al: Use of 320-detector computed tomographic angiography for infants and young children with congenital heart disease. *Pediatr Cardiol*, 2011; 32(4): 426–32
11. Hayabuchia Y, Inouea M, Watanabea N et al: Consideration of the pathological features of pediatric congenital heart diseases which are ideally suitable for diagnosing with multidetector-row CT. *Cardiol Res*, 2011; 2(4): 150–59
12. Paul JF, Rohnan A, Sigal-Cinqualbre A: Multidetector CT for congenital heart patients: What a paediatric radiologist should know. *Pediatr Radiol*, 2010; 40(6): 869–75
13. Hayabuchi Y, Inoue M, Watanabe N, Sakata M et al: Assessment of systemic-pulmonary collateral arteries in children with cyanotic congenital heart disease using multidetector-row computed tomography: Comparison with conventional angiography. *Int J Cardiol*, 2010; 138(3): 266–71
14. Ahmed S, Johnson PT, Fishman EK et al: Role of multidetector CT in assessment of repaired tetralogy of fallot. *Radiographics* 2013; 33: 1023–36
15. Stinn B, Stolzmann P, Fornaro J et al: Technical principles of computed tomography in patients with congenital heart disease. *Insights Imaging*, 2011; 2: 349–56
16. Ghanaati H, Tabib MA, Almasi A et al: Multidetector CT evaluation of congenital heart disease: A pictorial essay. *Iran J Radiol*, 2007; 4(4): 209–16
17. Dillman JR, Hernandez RJ: Role of CT in the evaluation of congenital cardiovascular disease in children. *Am J Roentgenol*, 2009; 192(5): 1219–31
18. Rajeshkannan R, Moorthy S, Pullara K et al: Role of 64-MDCT in evaluation of pulmonary atresia with ventricular septal defect. *Am J Roentgenol*, 2010; 194(1): 110–18
19. Gilkeson RC, Ciancibello L, Zahka K: Multidetector CT evaluation of congenital heart disease in pediatric and adult patients. *Am J Roentgenol*, 2003; 180(4): 973–80